

# NANOSAT CONSTELLATION MISSION DESIGN

Marco Concha and Robert DeFazio  
NASA Goddard Space Flight Center

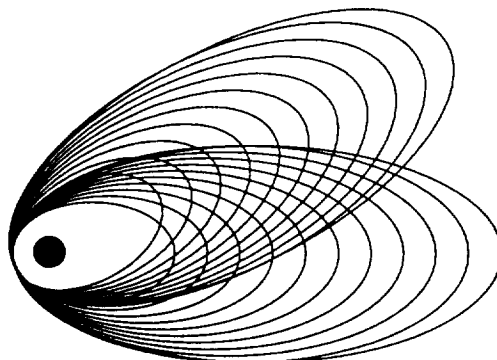
The NanoSat constellation concept mission proposes simultaneous operation of multiple swarms of as many as 22 identical 10 kg spacecraft per swarm. The various orbits in a NanoSat swarm vary from  $3 \times 12$  to  $3 \times 42 R_e$  in geometry. In this report the unique flight dynamics issues of this constellation satellite mission design are addressed. Studies include orbit design, orbit determination, and error analysis. A preliminary survey determined the orbital parameters that would limit the maximum shadow condition while providing adequate ground station access for three ground stations.

## Introduction

NanoSat is a mission class of spacecraft with the goal of placing multiple clusters of very small earth orbiting spacecraft into varying eccentric orbits. NASA's Goddard Space Flight Center (GSFC) is sponsoring the NanoSat concept as a means of spurring technology advancement in disciplines related to spacecraft development. The primary goal is to produce a 10 kg spacecraft capable of boosting itself to the mission orbit and performing a science gathering mission for one year. A summary of spacecraft requirements is listed in Table 1. The prototype mission would involve the simultaneous operation of multiple swarms of spacecraft. The baseline mission calls for 22 spacecraft per swarm. Proposed missions for such a constellation include surveys of the earth's magnetosphere and investigations of the Van Allen Belts. Such missions would benefit from the breadth of variation in altitude and Mean Local Time in a relatively short period.

With the objective of making spacecraft sub-systems better, cheaper and faster, a prototype mission scenario was defined in order to push GSFC's technology efforts beyond current levels. Preliminary analysis was performed in order to obtain an understanding of the mission's potential orbital characteristics. The results are intended to spur the iterative design process of the spacecraft and the mission class. This report summarizes mission design work to date.

Unlike typical earth orbiting constellation designs, the focus of NanoSat is not planetary observation, but space science in-situ measurement. Thus, unlike other constellation concepts, there is an emphasis on widely varying orbit geometry. Such a configuration would provide science opportunities at locations about the earth with a considerable variation in observation parameters. The project expressed interest in very high apogee radii as well. This emphasis places a limit on launching many spacecraft in varying orbit planes, as the energy cost (e.g. propulsion) becomes prohibitive. Therefore the spacecraft in each swarm is designed to share one orbit plane at deployment.



Two NanoSat swarms,  $\Delta\omega=30$   
Figure 1

Spacecraft Requirements	
Orbit	12 to 40 $R_e$ apogee, 3 $R_e$ perigee
Inclination	< 15 °
Orbital position knowledge	20 km
Mass	10 kg
Size	30 cm dia. x 10 cm height
Eclipse	475 min per orbit for 5 days

Table 1

Within each swarm, by incrementing the apogee radius by 3  $R_e$ , a total of 11 orbits are obtained ranging from 12 to 42  $R_e$ . Another early concept was to deploy multiple spacecraft per orbit, in the hopes of obtaining an efficient distribution of science data. For simplification purposes, a distribution of two spacecraft per orbit was chosen. The spacecraft are assumed to be deployed in half orbit separations. Thus, a total of 22 spacecraft per swarm is obtained. Likewise, a second swarm was prepared, separated by 30° in argument of perigee ( $\omega$ ), Figure 1. It is assumed that separate launch vehicles would deliver motherships for each swarm to a geosynchronous transfer orbit, 200 km x 6.6  $R_e$ . An apogee kick motor would then raise the perigee of each mothership to 3.0  $R_e$  while also maneuvering inclination and right ascension of the ascending node ( $\Omega$ ). Each NanoSat would use on board propulsion to raise apogee into its respective orbit.

For the analyses presented in this report, the following analytic parameters were used. The force model used was the JGM-2 21 x 21 truncated earth gravity model. Solar Radiation was modeled using a Coefficient of Reflectivity of 2.0. Both variation of parameter and Runge-Kutta analytical propagators were used to predict long term effects of the earth and moon gravity model perturbations. The cross-sectional area of each spacecraft is  $3.0 \times 10^{-8} \text{ km}^2$ .

As NanoSat matures in concept, undoubtedly requirements will change. However an effort was made in this mission design to quantify the environmental factors pertinent to spacecraft design. The preliminary studies presented herein are in response to concerns of the project spacecraft subsystems designers.

For such an ambitiously small spacecraft design, challenging constraints on power are imposed. Consequently, the first analysis performed was a survey of eclipse duration for the worst case orbits. Consideration of design criteria evolved from that analysis to the launch opportunities afforded by minimizing eclipse conditions. In response to the need for sizing the command, communication and control subsystems, an investigation into ground contact opportunities was initiated. As a follow on to these results a quick estimate of orbit determination accuracy was performed.

## Eclipse Duration

In studying the eclipse duration maximums of NanoSat spacecraft, it is assumed that the worst case conditions exist for orbits with small inclinations and the longest orbital periods, e.g. the 40  $R_e$  apogee case. Nonetheless it is helpful to examine the eclipse trends of other orbits in relation to various orbital parameters.

This study surveyed maximum eclipse duration for a variety of parameter values. Inclinations of 1.0°, 7.5°, and 15°; apogee radii of 12, 26, and 40  $R_e$ ; ascending nodes of 0, 90, 180, and 270°; and epochs of March 21, June 21, September 21, and December 21, 2008 at 00:00 GMT were all observed. For each combination of values, a one year propagation was conducted. The maximum eclipse duration for these parameters are presented in Figures 2-10. As expected, the 40  $R_e$  apogee radii for all three inclinations are the worst cases where the maximum eclipse duration exceeds 500 minutes (Figures 8, 9, 10). In most cases maximum eclipse duration occurs at  $\Omega$  values of either 0° or 180°. For these same high apogee orbits  $\Omega$  values of 90° or 270° reduce the maximum eclipse by about one half to under 300 minutes. When the apogee radius is reduced to 26  $R_e$  for a similar set of initial conditions, the maximum eclipses are upper bounded by 350 minutes with  $\Omega$ s of 0° and 180°, again, causing the largest eclipses. The cases for  $\Omega$ s of

90° and 270° show maximum eclipses less than or equal to 160 minutes. For an apogee radius of 12 R<sub>e</sub>, the values for bounding the maximum eclipse duration are 150 minutes and 90 minutes for Ω pairs of (0° and 180°) and (90° and 270°) respectively. From these cases it is concluded that choosing the Ω judiciously will permit the spacecraft design to incorporate the effects of a much lower maximum eclipse.

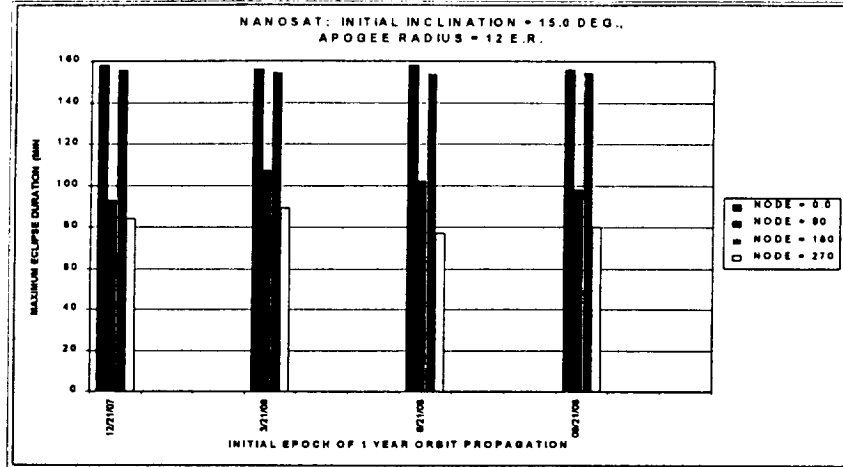


Figure 2

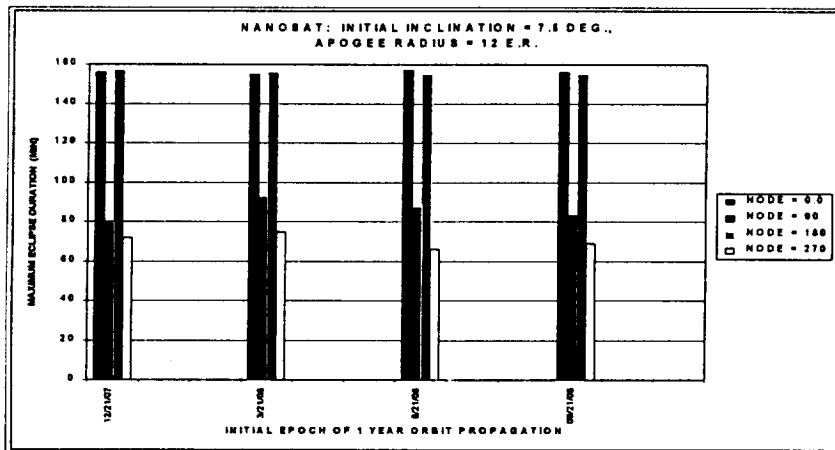


Figure 3

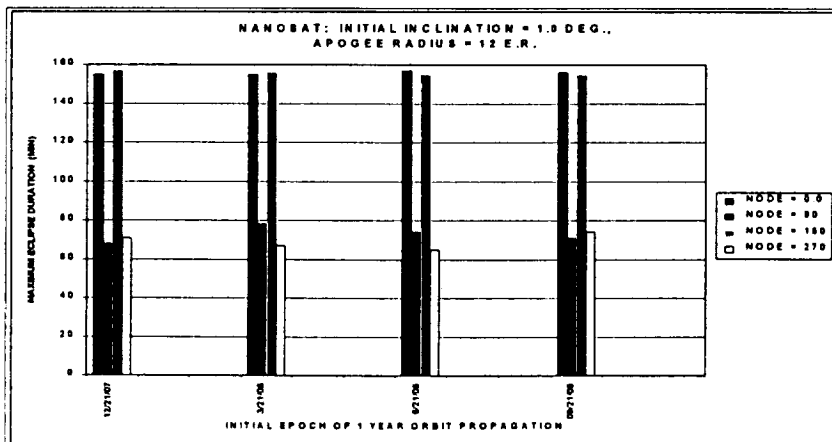


Figure 4

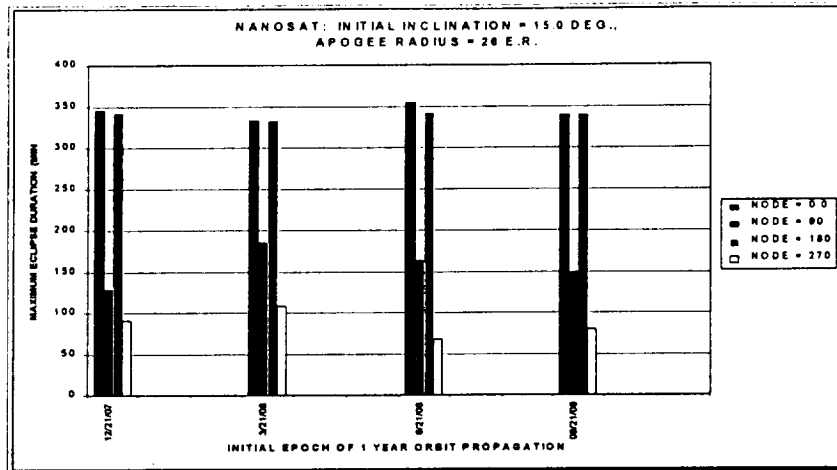


Figure 5

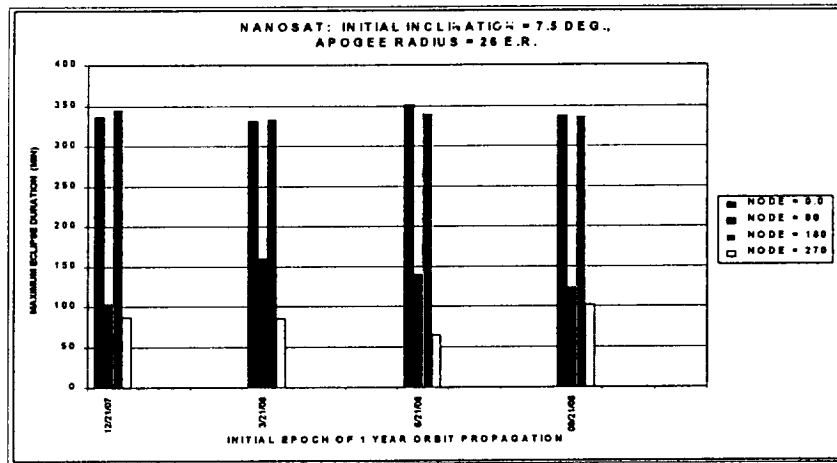


Figure 6

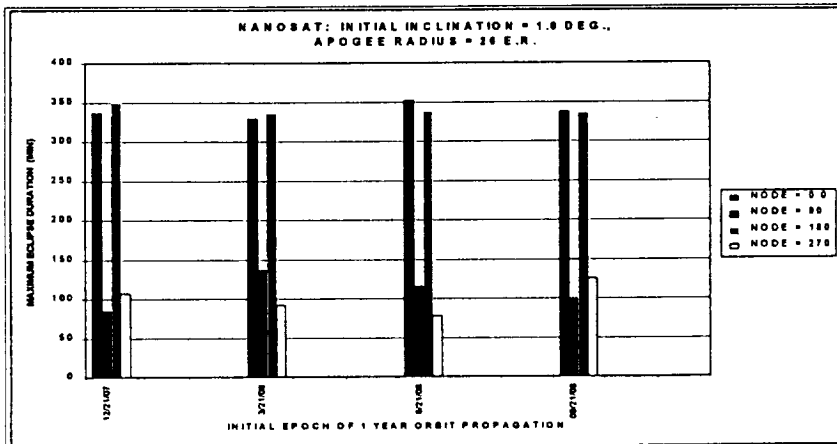


Figure 7

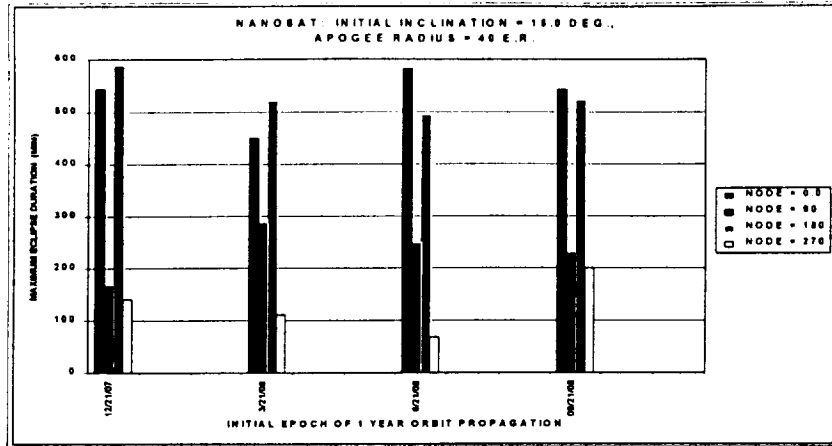


Figure 8

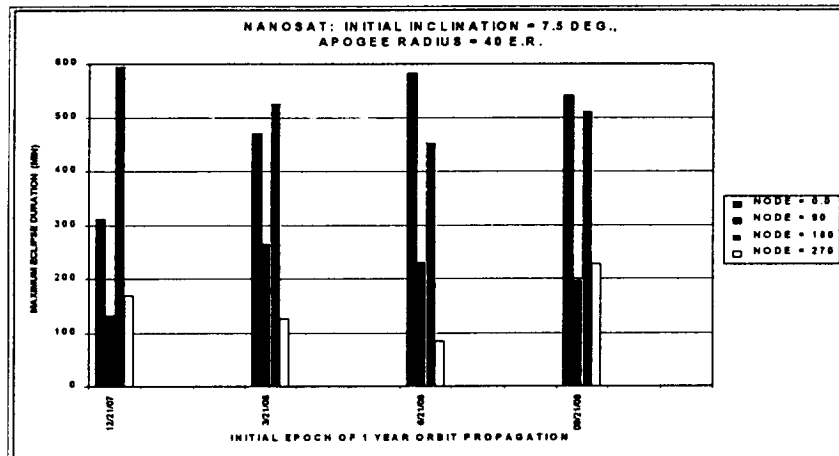


Figure 9

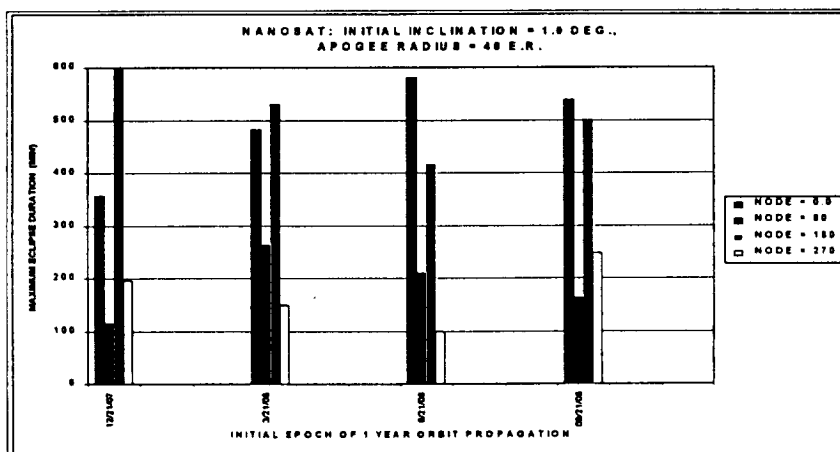


Figure 10

For spacecraft thermal control considerations, shadow conditions in excess of 400 minutes were deemed too conservative by subsystem engineers. Early power estimates established an eclipse restriction of 475 min per orbit for 5 days. These results show that these constraints can be managed, with compromise in initial orbital element selection. The  $\Omega$  cases for  $90^\circ$  and  $270^\circ$  are the most favorable and satisfy these constraints.

While the primary focus of this study was identifying eclipse trends, it is worthwhile to note the spacecraft state at the end of one year. Most notable is the orbit perturbation effect of the lunar gravity. The chief consequence of this effect is a large change in inclination for the high apogee orbits. Figure 11 shows the inclination history over the course of one year in the absence of correction maneuvers. Depending on the epoch, the inclination can increase as much as  $30^\circ$  over the course of a year in this configuration. This stands to reason as the  $40 R_e$  orbit semi-major axis is a significant percentage of the Earth-Moon distance (36% mean lunar distance), and therefore highly susceptible to lunar gravity orbit perturbations.

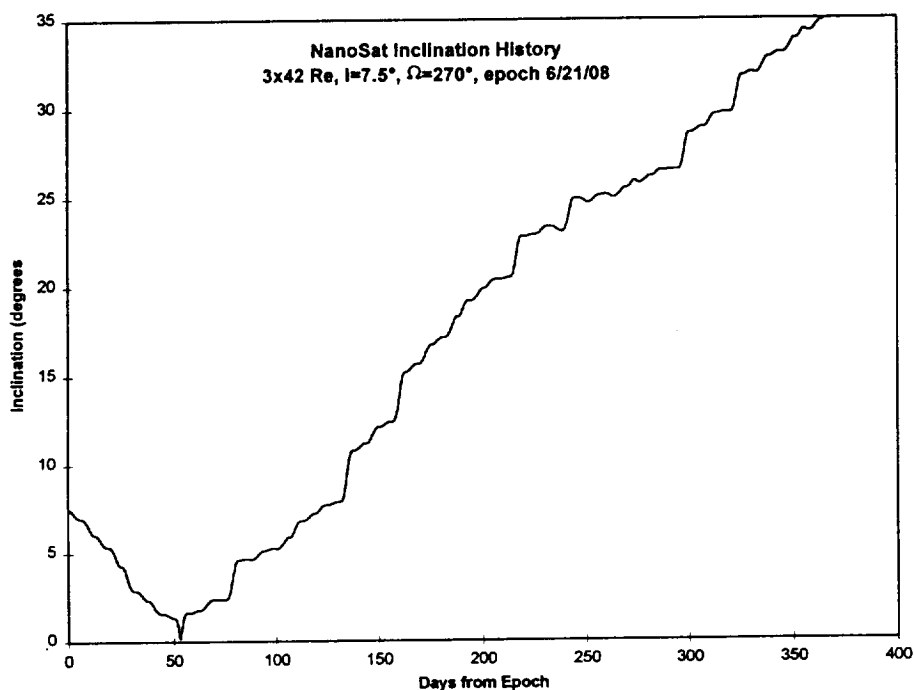


Figure 11

## Launch Opportunities

In consideration of the eclipse study results, an examination of launch opportunities over the course of one day was computed for inclination of  $7.5^\circ$ , apogee radius of  $40 R_e$ , and an epoch of June 21, 2008. As was shown in previous work (Figures 2-10) the summer solstice cases tended to have lower overall maximum eclipse values. Although the 15 degree inclination orbits yielded slightly better eclipse results over the course of one year, the  $7.5$  degree case was chosen in order to retain favorable field of view margin for payload instruments.

As before, the parameter of note for this one day study is  $\Omega$ . Due to the rotation of the earth,  $\Omega$  at launch varies by  $15^\circ$  per hour. Launch opportunities at 2 hour intervals were examined. In each case a 1 year propagation was performed to evaluate the maximum eclipse duration. For comparative purposes, another swarm was modeled by introducing a 30 degree difference in  $\omega$ , and generating another data set. Results are presented in Figure 12. The magnitude of the maximum eclipses followed the trend seen earlier

with the initial  $\Omega$ s near  $90^\circ$  and  $270^\circ$ : yielding smaller maximum eclipse durations than those with  $\Omega$ s near  $0^\circ$  and  $180^\circ$ .

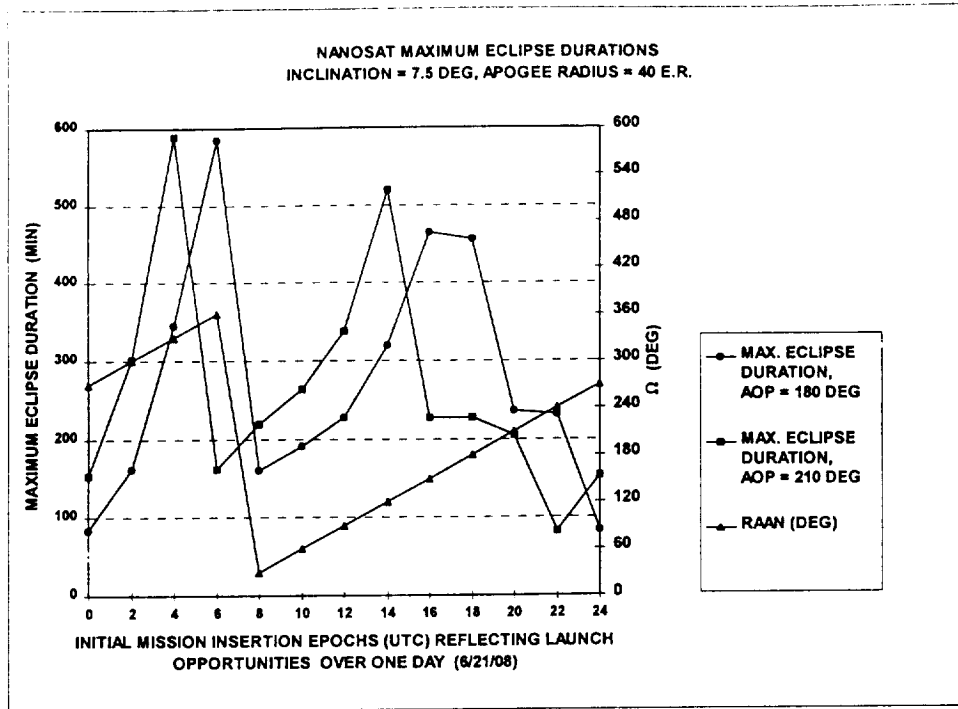


Figure 12

One last set of calculations for the NanoSat eclipses showed the distribution of eclipse durations over one year. For an initial  $\Omega$  of  $270^\circ$ , inclination of  $7.5^\circ$ , and an apogee radius of  $40 R_e$ , four different one year propagations were made each beginning with a different epoch, corresponding to equinoxes and solstices. Results are shown in Figures 13-16. The choice of  $\Omega$  at  $270^\circ$  tends to reduce the maximum eclipse for these conditions. The placement of the first local maximum for the eclipse seems to coincide approximately with the next equinox. Later local maximums do not necessarily hold to an equinox condition due to the orbit precession.

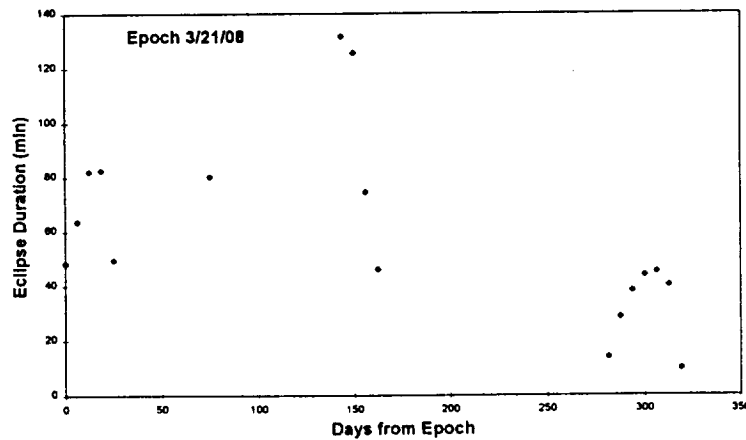


Figure 13

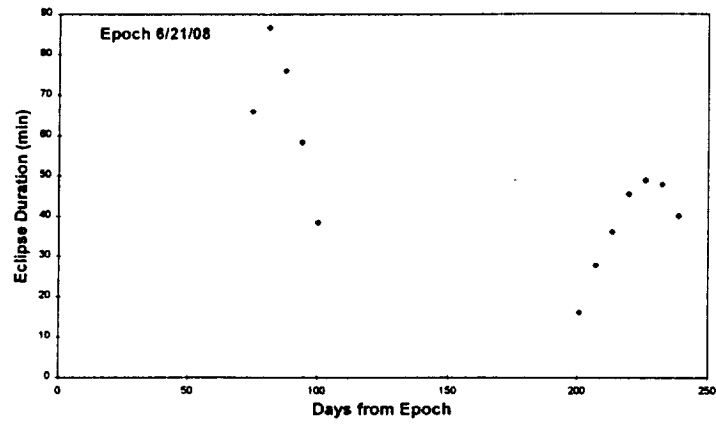


Figure 14

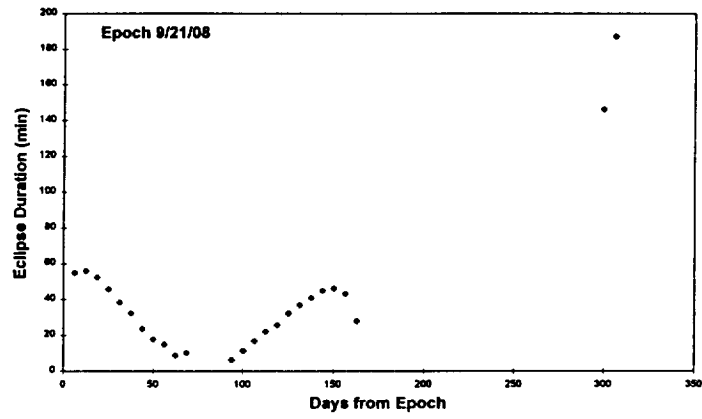


Figure 15

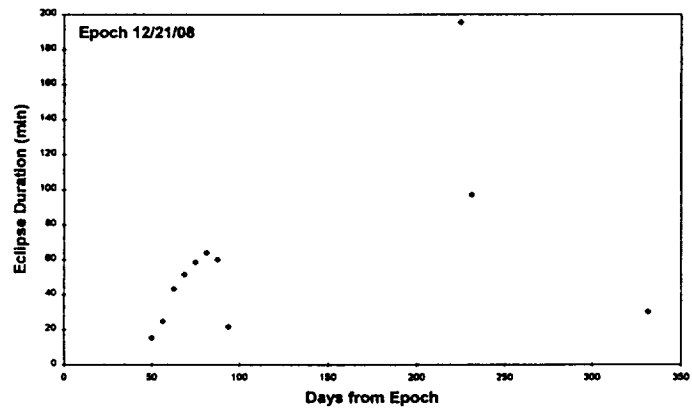


Figure 16

## Contact Survey

Using the eclipse and launch window analyses results, the prototypical set of orbits was selected for analyzing the ground station coverage for the entire NanoSat constellation. The two swarms prepared for the study were offset by  $30^\circ$  in  $\omega$ . Each swarm had  $\Omega$  of  $270^\circ$ , inclination of  $7.5^\circ$ , epoch of June 21, 2008 at 00:00:00 GMT. One swarm had an  $\omega$  of  $180^\circ$ , while the second swarm had an  $\omega$  of  $210^\circ$ . Each swarm consisted of 11 orbits. The two resident spacecraft in the  $3 \times 12 R_c$  were separated initially by  $180^\circ$  in mean anomaly. For each successive orbit, the next two spacecraft initial mean anomalies were incremented by  $15^\circ$ . These initial conditions were chosen in an attempt to pseudo-randomly distribute the swarm spacecraft. In total, 44 spacecraft were examined.

For providing typical global coverage, three ground station locations were selected. Antennas were placed at Goldstone, Madrid, and Canberra, each assuming a 5 degree elevation mask. Use of these facilities by NanoSat is not implied by their inclusion in this analysis. A slant range limit of  $5 R_c$  was used, to take into account the power limitations of the on board antenna.

Over the course of one year 11,500 passes were simulated over the three stations. In this period the busiest ground station coverage event was simultaneous contact with 12 spacecraft, which was highly anomalous. Figure 17 shows a 200 day history of simultaneous contacts sorted by station. This data was used by ground station schedulers to estimate the required data rates and storage specifications for NanoSat spacecraft. For the periods of high number of spacecraft contact, the lower orbits may be considered lower priority for link scheduling, as a download opportunity may be delayed for a relatively shorter period of time ( $3 \times 12$  period = 29 hours). In contrast, the high orbit periods consist of several days, ( $3 \times 42$  period = 6.25 days) offering long wait times in the event a link is not established.

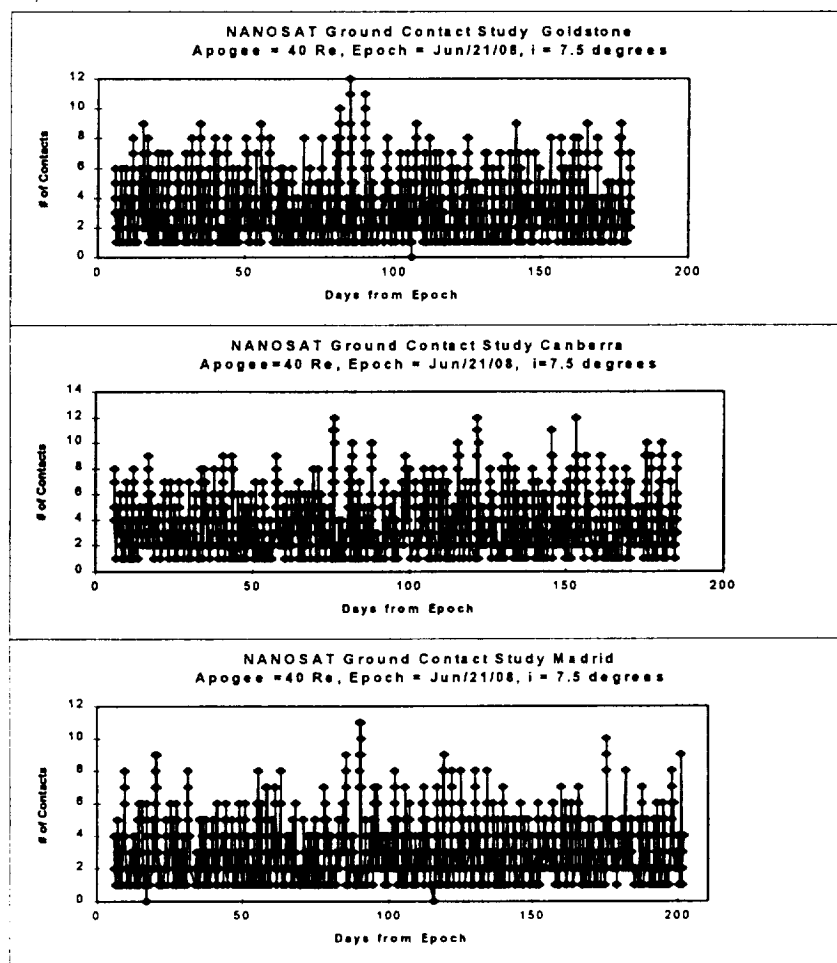


Figure 17

## **Orbit Determination / Error Analysis**

Setting the upper bound in error scenarios, the largest orbit is selected for the purpose of error analysis in orbit determination. The pass statistics generated in the last section were scheduled for the following scenario. A 40 R<sub>c</sub> apogee radius NanoSat contacts one ground station per pass and is propagated for the remainder of its period until contact is re-established. For the purposes of this analysis the assumption is that the time between passes equals the orbit period minus the contact time. For one ground station, this is not necessarily true for all cases. The assumption depends on the coverage of the other two ground stations. Contact times will also vary in length, therefore a survey of possible contact times between one ground station and one spacecraft using Doppler range-rate measurements was conducted. Since the period of this orbit is much greater than any of the contact passes, there is no significant variance in orbit determination error. A pass duration of 120 minutes yields a total position error of 19.2 km, total velocity error of .388 meters/sec. A pass duration of 300 minutes yields a total position error of 18.9 km, total velocity error of .380 meters/sec. The larger duration passes are available when slant range constraints are loosened, however there is no appreciable advantage using this technique since the predominant source of error in these ranges is the contribution of tropospheric refraction of the measurement.

## **Conclusions**

From the survey of orbital parameters conducted in this report, a workable set of design options is obtained. A feasible orbit design, though preliminary, may be selected given the constraints of the mission. In order to minimize the maximum eclipse duration for the longest orbit period, right ascension of ascending node of 270° is recommended. By selecting a launch epoch near June 21, 2008 and scrutinizing Figure 10 for best launch opportunities over the course of one day, one year maximum shadow conditions can be designed well within spacecraft requirements. A one year mission is feasible with the current requirements, if large inclinations at high orbits can be accepted. A ground system must be designed to accommodate several simultaneous contacts over the course of one year, where the maximum observed can be 12 spacecraft. Orbit determination error can nominally provide a state within 20 km of accuracy for the largest orbits.

The results reported in this survey were generated using Analytical Graphics Inc.'s Satellite Tool Kit software, version 4.0. The Goddard Space Flight Center's Goddard Mission Analysis System (GMAS) and Orbit Determination Error Analysis System (ODEAS) were also used.

## **Acknowledgments**

The authors would like to thank the following for their significant contribution to this report, Michael Mesarch, Lauri Newman, and Mark Woodard of the Goddard Space Flight Center.

Marco Concha

Guidance, Navigation, and Control Center  
NASA/Goddard Space Flight Center  
Greenbelt, Maryland 20771

Robert DeFazio